Synthesis and Structures of Mono(1-aza-allyl) Complexes of Aluminum[†]

Chunming Cui,[‡] Herbert W. Roesky,*,[‡] Mathias Noltemeyer,[‡]
Michael F. Lappert,[§] Hans-Georg Schmidt,[‡] and Haijun Hao[‡]

*Institut für Anorganische Chemie der Universität Göttingen, Tammannstrasse 4,
D-37077 Göttingen, Germany, and University of Sussex, Brighton, BN1 9QJ, U.K.*

The synthesis and structures of new aluminum complexes using the 1-aza-allyl ligand R (R = [N(SiMe$_3$)C(Ph)C(SiMe$_3$)$_2$]$^-$) are described. The reaction of RLi·THF with AlMe$_2$Cl, AlMeCl$_2$, AlCl$_3$, and AlBr$_3$ in diethyl ether or *n*-hexane, after workup, afforded RAlMe$_2$ (**1**), RAlMeCl (**2**), RAlCl$_2$ (**3**), and RAlBr$_2$ (**4**), respectively, while [RAlF(μ-F)]$_2$ (**5**) or RAlI$_2$ (**6**) was prepared in high yield by the reaction of RAlMe$_2$(**1**) with 2 equiv of Me$_3$SnF or I$_2$, respectively, in toluene. The complex **2** or **3** reacts with an excess of THF to give the corresponding THF adduct RAlClMe·THF (**7**) or RAlCl$_2$·THF (**8**). Compounds **7** and **8** are not stable; the coordinated THF can be easily removed in vacuo at ambient temperature. The molecular structures of **3**, **5**, and **8** have been established by X-ray crystallography. Compound **3** is a monomer with a chelating η^3 1-aza-allyl ligand, while compound **8** forms an open structure with an η^1 pendant ligand. Compound **5** is the first example of a dimeric aluminum difluoride, in which two bridging F atoms reside on the pseudo 2-fold axis of the approximately C_2 symmetric molecule. The two pentacoordinated aluminum atoms can be described as having distorted trigonal-bipyramidal geometries, which have in common one bridging F atom in an apical position and the other bridging F atom in an equatorial position.

Introduction

Major advances have been achieved in the polymerization of olefins by single-site catalysts. The majority of these catalysts are metallocene derivatives of group 4. However, Bochmann and Dawson[1] and Coles and Jordan[2] recently reported the application of cationic aluminum alkyl species for olefin polymerization reactions to generate high molecular weight polyolefins. As is the case of metallocenes of group 4, the stability of cationic aluminum species will highly depend on the ancillary ligand set and the choice of the counteranion.[3−5]

We have been interested in aluminum complexes used in catalysis[6] and are interested in developing the chemistry of active aluminum species with monoanionic, chelating spectator ligands. The modification of the steric and electronic properties at the aluminum center consequently will control the properties of the catalytic site. Aluminum complexes containing bulky amidinates have been extensively studied and have been used to generate three-coordinate cationic species.[2,7] However, base-free cationic sites have not been obtained using these ligands.[2,8] Interest in fundamental studies of the relationships between ligand structure and metal coordination geometry prompted us to extend the use of this methodology to the synthesis of aluminum complexes containing the bulky 1-aza-allyl ligand [N(SiMe$_3$)C(Ph)C-(SiMe$_3$)$_2$]$^-$.[9] The known 1-aza-allyl complexes are rare; only a few main group (K, Li, Pb, Sn) and transition metal (Cu, Hg, Zr, Sm, Yb, Th) complexes have been reported.[9−14] To the best of our knowledge, aluminum complexes having 1-aza-allyl ligands are not known; the only related compounds reported are bis[2-C(SiMe$_3$)$_2$-Py]$_2$AlCl and its corresponding cation.[15] Herein, we report the general preparative routes for the synthesis of mono(1-aza-allyl) aluminum dialkyls and the related dihalides using the bulky 1-aza-allyl [N(SiMe$_3$)C(Ph)C-(SiMe$_3$)$_2$]$^-$ ligand.

[†] Dedicated to Professor Yu. A. Buslaev on the occasion of his 70th birthday.
[‡] Universität Göttingen.
[§] University of Sussex.
(1) Bochmann, M.; Dawson, D. M. *Angew. Chem.* **1996**, *108*, 2371; *Angew. Chem., Int. Ed. Engl.* **1996**, *35*, 2226.
(2) Coles, M. P.; Jordan, R. F. *J. Am. Chem. Soc.* **1997**, *119*, 8125.
(3) Jordan, R. F. *Adv. Organomet. Chem.* **1991**, *32*, 325.
(4) Hlatky, G. G.; Turner, H. W.; Eckman, R. R. *J. Am. Chem. Soc.* **1989**, *111*, 2728.
(5) Chen, Y. H.; Metz, M. V.; Li, L.; Stern, C. L.; Marks, T. J. *J. Am. Chem. Soc.* **1998**, *120*, 6287.
(6) Storre, J.; Schnitter, C.; Roesky, H. W.; Schmidt, H.-G.; Noltemeyer, M.; Fleischer, R.; Stalke, D. *J. Am. Chem. Soc.* **1997**, *119*, 7505.
(7) Coles, M. P.; Swenson, D. C.; Jordan, R. F.; Young, V. G. *Organometallics* **1997**, *16*, 5183.

(8) Ihara, E.; Young, V. G.; Jordan, R. F. *J. Am. Chem. Soc.* **1998**, *120*, 8277.
(9) Hitchcock, P. B.; Lappert, M. F.; Layh, M. *Inorg. Chim. Acta* **1998**, *269*, 181.
(10) Hitchcock, P. B.; Lappert, M. F.; Layh, M. *J. Chem. Soc., Dalton Trans.* **1998**, 1619.
(11) Hitchcock, P. B.; Lappert, M. F.; Tian, S. *J. Chem. Soc., Chem. Commun.* **1994**, 2637.
(12) Hitchcock, P. B.; Hu, J.; Lappert, M. F.; Layh, M.; Severn, J. *J. Chem. Soc., Chem. Commun.* **1997**, 1189.
(13) Armstrong, D. R.; Clegg, W.; Dunbar, L.; Liddle, S. T.; Mac-Grogor, M.; Mulvey, R. E.; Reed, D.; Quiss, S. A. *J. Chem. Soc., Dalton Trans.* **1998**, 3431.
(14) Lappert, M. F.; Layh, M. *Tetrahedron Lett.* **1998**, *39*, 4745.
(15) Engelhardt, L. M.; Kynast, U.; Raston, C. L.; White, A. H. *Angew. Chem.* **1987**, *99*, 702; *Angew. Chem., Int. Ed. Engl.* **1987**, *26*, 681.

Experimental Section

General Procedures. All manipulations were performed on a high-vacuum line or in a glovebox under a purified N_2 atmosphere. Solvents were distilled from Na/benzophenone ketyl prior to use, except for pentane, which was distilled from potassium. Chemicals were purchased from Aldrich and used as received, except for $AlCl_3$ and $AlBr_3$, which were sublimed in vacuo prior to use. Trimethytin fluoride[16] and [N(SiMe₃)C-(Ph)C(SiMe₃)₂]Li·THF[9,14] were prepared as described in the literature.

Elemental analyses were performed by the Analytisches Labor des Instituts für Anorganische Chemie der Universität Göttingen. Bruker AM 200 and Bruker AM 250 spectrometers were used to record ¹H NMR (250.130 MHz), ¹³C NMR (100.600 MHz), ¹⁹F NMR (235.320 MHz), ²⁷Al NMR (104.245 MHz), and ²⁹Si NMR (79.460 MHz) spectra. The chemical shifts were externally referenced to SiMe₄ (¹H, ¹³C, ²⁹Si), CFCl₃ (¹⁹F), and AlCl₃ (²⁷Al), respectively. EI (70 eV) mass spectra were measured on Finnigan MAT 8230 or Varian MAT CH5 instrument. Melting points were measured in sealed glass tubes and were not corrected.

RAlMe₂ (1). AlMe₂Cl (10 mL, 1 M in *n*-hexane, 10 mmol) was added to a stirred suspension of RLi·THF (4.14 g, 10 mmol) in diethyl ether (30 mL) at −78 °C. The mixture was allowed to warm to room temperature and stirred for an additional 15 h. The volatiles were removed in vacuo, the crude product was extracted with pentane (30 mL), and the extract was concentrated to dryness in vacuo. Pure samples of **1** were obtained by sublimation (65 °C, 0.005 mbar) (3.5 g, 85%). Mp: 60−62 °C. ¹H NMR (C₆D₆): δ −0.19 (s, 6H, AlMe₂), −0.06 (s, 9H, NSiMe₃), 0.20 (s, 18H, SiMe₃), 6.90−7.00 (m, 3H, Ph), 7.25 (d, 2H, Ph). ¹³C NMR (C₆D₆): δ −5.50 (br s, AlMe₂), 0.83 (s, NSiMe₃), 3.61(s, SiMe₃), 49.5 (s, CSi₂), 127.1, 128.1, 130.3 (s, Ph), 143.1 (s, *ipso*-C), 208.5 (s, CN). ²⁹Si NMR (C₆D₆): δ −4.11 (s, SiMe₃), 15.7 (s, NSiMe₃). ²⁷Al NMR (C₆D₆): δ 161.2 ($\nu_{1/2}$ = 2920 Hz). MS: *m/e* (%): 391 (M⁺), 376 (M⁺ − Me). Anal. Calcd for C₁₉H₃₈AlNSi₃ (391.75): C, 58.25; H, 9.78; N, 3.57. Found: C, 58.23; H, 9.41; N, 3.74.

RAlMeCl (2). AlMeCl₂ (3 mL, 1 M in *n*-hexane, 3 mmol) was added to a suspension of RLi·THF (1.24 g, 3 mmol) in *n*-hexane (20 mL) at −78 °C. The reaction mixture was allowed to warm to room temperature and was stirred for 15 h. A colorless precipitate was filtered, and volatiles were removed. The crude product was sublimed (70 ˚C, 0.002 mbar) to give analytically pure solid of **2** (0.96 g, 78%). Mp: 120−122 °C. ¹H NMR (C₆D₆): δ −0.03 (s, 9H, NSiMe₃), −0.01 (s, 3H, AlCH₃), 0.18 (d, 18H, SiMe₃), 6.83−6.96 (m, 3H, Ph), 7.22 (d, 2H, Ph). ¹³C NMR (C₆D₆): δ −5.7 (br s, AlCH₃), 0.60 (s, NSiMe₃), 2.98, 3.41 (s, SiMe₃), 53.5 (s, CSi₂), 126.7, 128.0, 130.5 (s, Ph), 141.9 (s, *ipso*-C), 210.1 (s, CN). ²⁷Al NMR (C₆D₆): δ 138.8 ($\nu_{1/2}$ = 2120 Hz). MS: *m/e* (%) 411 (M⁺), 396 (M⁺ − Me), 376 (M⁺ − Cl, 4). Anal. Calcd for C₁₈H₃₅AlClNSi₃ (412.17): C, 52.23; H, 8.56; N, 3.34. Found: C, 51.63; H, 8.55; N, 2.94.

RAlCl₂ (3). A solution of RLi·THF (0.83 g, 2 mmol) in *n*-hexane (20 mL) was added to a stirred suspension of AlCl₃ in *n*-hexane (10 mL) at −78 °C. The mixture was allowed to warm to room temperature and stirred for 15 h. After filtration to remove LiCl, the solvent was removed in vacuo and the residual was pumped in vacuo (0.01 mbar) for 4 h. The crude product was crystallized from *n*-hexane (−8 °C) to give colorless crystals (0.73 g, 84%). Mp: 170 °C dec. ¹H NMR (C₆D₆): δ 0.00 (s, 9H, NSiMe₃), 0.24 (s, 18H, SiMe₃), 6.85−6.95 (m, 3H, Ph), 7.23 (d, 2H, Ph). ¹³C NMR (C₆D₆): δ 0.65 (s, NSiMe₃), 3.16 (s, SiMe₃), 54.6 (s, CSi₂), 126.6, 128.4, 131.1(s, Ph), 140.7 (s, *ipso*-C), 212.8 (s,CN). ²⁹Si NMR (C₆D₆): δ −1.14 (br s, SiMe₃), 9.72 (s, NSiMe₃). ²⁷Al NMR (C₆D₆): δ 111.5 ($\nu_{1/2}$ = 772 Hz). MS: *m/e* (%) 431 (M⁺), 416 (M⁺ − Me). Anal. Calcd for C₁₇H₃₂AlCl₂NSi₃ (432.56): C, 47.20; H, 7.45; N, 3.24. Found: C, 47.46; H, 7.51; N, 3.17.

(16) Krause, E. *Ber. Dtsch. Chem. Ges.* **1918**, *51*, 1447.

RAlBr₂ (4). This compound was prepared using the same procedure described for **3**, RLi·THF (0.62 g, 1.5 mmol) in *n*-hexane (15 mL) and AlBr₃ (0.40 g, 1.5 mmol) in *n*-hexane (5 mL). The crude product was crystallized from *n*-hexane to give colorless crystals (0.48 g, 61%). Mp: 105 °C. ¹H NMR (C₆D₆): δ 0.02 (s, 9H, NSiMe₃), 0.27 (s, 18H, SiMe₃), 6.80−6.95 (m, 3H, Ph), 7.25 (d, 2H, Ph). ¹³C NMR (C₆D₆): δ 0.85 (s, NSiMe₃), 3.54 (s, SiMe₃), 41.0 (s, CSi₂), 126.6, 128.6, 131.2 (s, Ph), 140.7 (s, *ipso*-C), 212.4 (s, CN). ²⁹Si NMR (C₆D₆): δ −1.02 (s, SiMe₃), 10.3 (s, NSiMe₃). ²⁷Al NMR (C₆D₆): δ 107.8 ($\nu_{1/2}$ = 875 Hz). MS: *m/e* (%): 521 (M⁺), 506 (M⁺ − Me), 422 (M⁺ − Br, 15). Anal. Calcd for C₁₇H₃₂AlBr₂NSi₃ (521.48): C, 39.15; H, 6.18; N, 2.68. Found: C, 39.22; H, 6.47; N, 2.99.

[RAlF(μ-F)]₂ (5). Toluene (20 mL) was added to a mixture of **1** (0.55 g, 1.4 mmol) and Me₃SnF (0.48 g, 2.8 mmol) at room temperature. The mixture was stirred for 15 h, resulting in a clear solution. All volatiles were removed in vacuo to leave a white solid, which was crystallized from toluene/*n*-hexane (1: 10) and stored at −20 °C for 2 days to afford colorless crystals (0.35 g, 63%). Mp: 185 °C dec. ¹H NMR (C₆H₆): δ 0.14 (s, 9H, NSiMe₃), 0.41 (br s, 18H, SiMe₃), 6.87−7.00 (m, 3H, Ph), 7.32 (d, 2H, Ph). ¹H NMR (toluene-*d₈*, 303 K): δ 0.13 (s, 9H, NSiMe₃), 0.35 (s, 18H, SiMe₃), 7.01−7.09 (m, 3H, Ph), 7.32 (d, 2H, Ph). ¹H NMR (toluene-*d₈*, 213 K): δ 0.60 (s, SiMe₃), 0.28 (s, SiMe₃), 0.18 (s, NSiMe₃), 0.14 (s, NSiMe₃), Ph was not recorded. ¹H NMR(toluene-*d₈*, 193 K): δ 0.15 (s, NSiMe₃), 0.20 (s, NSiMe₃), 0.31 (s, SiMe₃), 0.62 (s, SiMe₃), 6.81 (m,Ph), 6.93 (m,Ph), 7.27 (d, Ph), 7.34 (d,Ph). ¹³C NMR (C₆H₆): δ 0.63 (s, NSiMe₃), 2.98 (s, SiMe₃), 40.9 (s, CSi₂), 125.7, 128.4, 131.1 (s, Ph), 147.2 (s, *ipso*-C), 212.8 (s, CN). ¹⁹F NMR (C₆D₆): δ −160.2 (br s, $\nu_{1/2}$ = 400 Hz). ¹⁹F NMR (toluene-*d₈*, 293 K): δ −160.6 (br s, $\nu_{1/2}$ = 400 Hz). ¹⁹F NMR (toluene-*d₈*, 258 K): δ −160.3 (s), −159.5 (s), −140.4 (br s, $\nu_{1/2}$ = 180 Hz), −132.6 (br s, $\nu_{1/2}$ = 140 Hz), −120.5 (s br, $\nu_{1/2}$ = 180 Hz). ¹⁹F NMR (toluene-*d₈*, 213 K): δ −159.7 (t, 0.8F, *J* = 15.0 Hz), −158.4 (t, 1.2F, *J* = 13.4 Hz), −141.1 (d, 0.4F, *J* = 82.4 Hz), −133.3 (s, 1.2F), −120.6 (d, 0.4F, *J* = 81.9 Hz). Anal. Calcd for C₃₄H₆₄Al₂F₄N₂Si₆ (799.34): C, 51.09; H, 8.07; N, 3.50. Found: C, 50.67; H, 7.69; N, 3.22.

RAlI₂ (6). A solution of **1** (4.02 g, 10.3 mmol) in toluene (20 mL) was added to a solution of I₂ (5.25 g, 20.6 mmol) in toluene (40 mL) at room temperature. The mixture was stirred for 18 h at room temperature, resulting in a slightly brown-yellow solution. All volatiles were removed in vacuo, the residual was extracted with *n*-hexane (2 × 60 mL), and the extract was concentrated and stored at −20 °C overnight to give slightly yellow crystals, which were collected by filtration and dried (5.2 g, 92%). Mp: 84−85 °C. ¹H NMR (C₆D₆): δ 0.06 (s, 9H, NSiMe₃), 0.30 (s, 18H, SiMe₃), 6.85−6.94 (m, 3H, Ph), 7.21 (d, 2H, Ph). ¹³C NMR (C₆D₆): δ 1.25 (s, NSiMe₃), 4.22 (s, SiMe₃), 41.95 (s, CSi₂), 126.1, 128.4 and 131.3 (s, Ph), 140.8 (s, *ipso*-C), 211.7 (s, CN). ²⁹Si NMR (C₆D₆): δ −0.96 (s, SiMe₃), 11.1 (s, NSiMe₃). ²⁷Al NMR (C₆D₆): δ 80.1. MS: *m/e* (%) 615 (M⁺, 1.6), 600 (M⁺ − Me), 488 (M⁺ − I). Anal. Calcd for C₁₇H₃₂AlI₂NSi₃ (615.57): C, 33.14; H, 5.24; N, 2.27. Found: C, 32.72; H, 5.42; N, 2.04.

RAlMeCl·THF (7). **2** (0.20 g, 0.48 mmol) was dissolved in THF (5 mL). After 30 min of stirring at room temperature, the excess THF was removed in vacuo. The crude product was crystallized from pentane to give colorless crystals (0.20 g, 85%). Mp: 45−46 °C. ¹H NMR (C₆D₆): δ −0.14 (s, 3H, AlCH₃), 0.12 (s, 9H, NSiMe₃), 0.23 (br s, 18H, SiMe₃), 1.17 (m, 4H, THF), 3.48 (m, 4H, THF), 6.88−6.98 (m, 3H, Ph), 7.28−7.35 (d, 2H, Ph). ¹³C NMR (C₆D₆): δ −6.0 (s, AlCH₃), 0.81, 1.69 (s, NSiMe₃), 3.44 (s, SiMe₃), 25.3 (s, THF), 41.2 (s, CSi₂), 69.6 (s, THF), 126.2, 128.8, 129.8 (s, Ph), 144.7 (s, *ipso*-C), 196.0 (s, CN). ²⁷Al NMR (C₆D₆): δ 130.2 ($\nu_{1/2}$ = 980 Hz). Anal. Calcd for C₂₂H₄₃AlClNOSi₃ (484.17): C, 54.54; H, 8.88; N, 2.89. Found: C, 54.17; H, 8.62; N, 3.13.

RAlCl₂·THF (8). This compound was prepared using **3** (0.43 g, 1 mmol) and THF (10 mL) as described for **7.** After workup,

Table 1. Summary of Crystal Data for Complexes 3, 5, and 8

	3	5	8
formula	$C_{17}H_{32}AlCl_2NSi_3$	$C_{37}H_{71}Al_2F_4N_2Si_6$ incl. 0.5 hexane	$C_{21}H_{40}AlCl_2NOSi_3$
fw	432.59	842.46	504.69
temp (K)	150(2)	200(2)	203(2)
cryst syst	orthorhombic	triclinic	monoclinic
space group	*Pbca*	*P*$\bar{1}$	*P*$2_1/c$
a (Å)	16.895(2)	10.916(3)	14.290(2)
b (Å)	16.129(2)	13.712(6)	11.217(2)
c (Å)	17.769(2)	18.242(6)	18.358(3)
α (deg)	90	79.13(3)	90
β (deg)	90	80.207(13)	98.268(11)
γ (deg)	90	69.784(15)	90
V (Å^3)	4842.3(10)	2499.9(15)	2912.1(9)
Z	8	2	4
d(calcd) (Mg/m^3)	1.187	1.119	1.151
abs coeff (mm^{-1})	0.454	0.243	0.389
$F(000)$	840	906	1080
cryst size (mm)	$0.70 \times 0.40 \times 0.20$	$0.50 \times 0.50 \times 0.50$	$0.60 \times 0.60 \times 0.50$
θ range (deg)	3.56−25.05	3.55−20.04	3.63−21.95
limiting indices	$-18 \leq h \leq 20$ $-19 \leq k \leq 19$ $-21 \leq l \leq 19$	$-10 \leq h \leq 10$ $-13 \leq k \leq 13$ $-17 \leq l \leq 17$	$-15 \leq h \leq 15$ $-8 \leq k \leq 11$ $-16 \leq l \leq 19$
no. of reflns collected	10 178	8628	3809
no. of indep reflns	4273 ($R_{int} = 0.0502$)	4653 ($R_{int} = 0.0498$)	3519 ($R_{int} = 0.1363$)
no. of data/restraints/params	4266/0/226	4634/319/493	3500/0/271
GOF/F^2	1.091	1.040	1.063
R indices [$I > 2\sigma(I)$]	$R1 = 0.0380$ $wR2 = 0.0844$	$R1 = 0.0493$ $wR2 = 0.1130$	$R1 = 0.0518$ $wR2 = 0.1100$
R indices (all data)	$R1 = 0.0590$ $wR2 = 0.1007$	$R1 = 0.0744$ $wR2 = 0.1390$	$R1 = 0.0518$ $wR2 = 0.1384$
largest diff peak/hole (e Å^{-3})	0.361/−0.231	0.272/−0.323	0.266/−0.258

colorless crystals (0.45 g, 89%) were obtained from *n*-hexane at −8 °C. Mp: 88−89 °C. ^{1}H NMR (C_6D_6): δ 0.16 (s, 9H, NSiMe$_3$), 0.28 (s, 18H, SiMe$_3$), 1.16 (m, 4H, THF), 3.55 (m, 4H, THF), 6.84−6.95 (m, 3H, Ph), 7.32 (d, 2H, Ph). ^{13}C NMR (C_6D_6): δ 1.00 (s, NSiMe$_3$), 2.96 (s, SiMe$_3$), 25.7 (s, THF), 40.9 (s, CSi$_2$), 67.9 (s, THF), 126.2, 128.6, 129.9 (s, Ph), 147.3 (s, *ipso*-C), 182.1 (s, CN). ^{29}Si NMR (C_6D_6): δ −6.18 (s, SiMe$_3$), 1.68 (s, NSiMe$_3$). ^{27}Al NMR (C_6D_6): δ62.66 ($\nu_{1/2}$ = 5600 Hz). Anal. Calcd for $C_{21}H_{40}AlCl_2NOSi_3$ (504.69): C, 49.98; H, 7.99; N, 2.77. Found: C, 49.38; H, 8.06; N, 2.66.

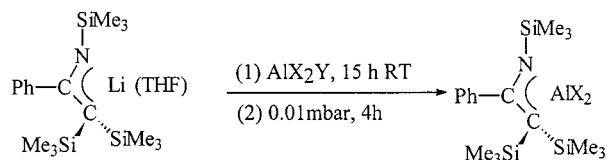**X-ray Structure Determinations and Refinements.** Data for crystal structures of **3**, **5**, and **8** were collected on a Stoe-Siemens four-circle diffractometer using Mo Kα radiation (λ = 0.710 73 Å). All structures were solved by direct methods (SHELXS-96)[17] and refined against F_2 using SHELXL-97.[18] All heavy atoms were refined anisotropically. Hydrogen atoms were included using the riding model with U_{iso} tied to the U_{iso} of the parent atom. Crystal data, data collection details, and solution and refinement procedures are summarized in Table 1.

Results and Discussions

Synthesis of Aluminum 1-Aza-allyl Complexes. The reaction of RLi·THF with AlMe$_2$Cl, AlMeCl$_2$, AlCl$_3$, and AlBr$_3$ in ether or *n*-hexane, after workup, afforded RAlMe$_2$ (**1**), RAlMeCl (**2**), RAlCl$_2$ (**3**), and RAlBr$_2$ (**4**), respectively, in high yield (Scheme 1). Initially these products are in equilibrium with their corresponding THF adducts, which was confirmed by the ^{1}H NMR analysis. However, solvent-free compounds can be easily obtained by sublimation in high-vacuum or pumping the crude products for a prolonged time in high vacuum at ambient temperature. Finally, crystallization from *n*-hexane yielded solvent-free products. On the other hand,

(17) Sheldrick, G. M. *Acta Crystallogr.* **1990**, *A46*, 467.
(18) Sheldrick, G. M. *SHELXL, Program for Crystal Structure Refinement;* University of Göttingen: Göttingen, Germany, 1997.
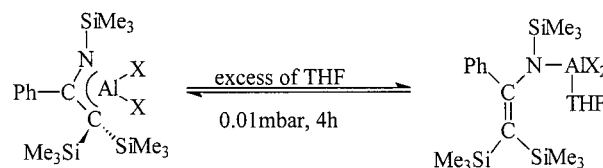
Scheme 1

Y = Cl, X = Me (**1**); Me, Cl (**2**); Cl (**3**)

Y = Br, X = Br (**4**)

Scheme 2

X = Cl, Me (**7**)

X = Cl   (**8**)

THF adducts can be easily prepared by dissolving compounds **1**−**4** in an excess of THF. According to this procedure, we prepared the adducts RAlMeCl·THF (**7**) and RAlCl$_2$·THF (**8**) (Scheme 2). Both compounds are not stable; they are easily oxidized and hydrolyzed on exposure to air, as indicated by an immediate color change from colorless to red. The different stabilities of compounds **1**−**4** and their corresponding THF adducts can be explained by the different bonding modes of the ligand, as demonstrated by the X-ray structure analyses of compound **3** and **8**. The solvents seem to be important for the synthesis of compounds **1**−**4**. Complex **1** can be obtained in ether in high yield (85−98%), but for **2**−**4**,
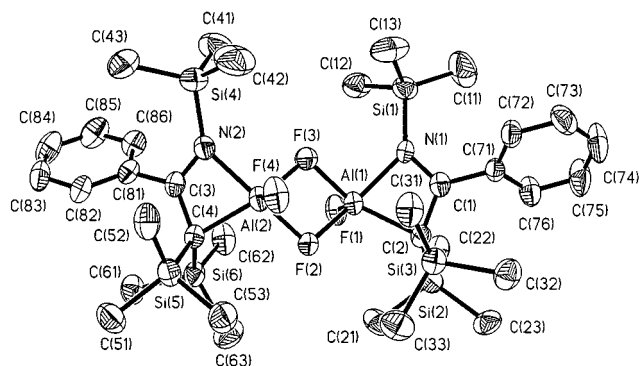
the synthesis in ether resulted in low yields (around 20%). The same reactions in *n*-hexane gave satisfactory yields (61−84%) for all compounds.

The reaction of RAlMe$_2$ (**1**) with 2 equiv of Me$_3$SnF in toluene yielded the dimeric difluoride [RAlF(μ-F)]$_2$ (**5**, eq 1), while the reaction of **1** with 2 equiv of I$_2$ in toluene at room temperature generated the diiodide, RAlI$_2$ (**6**, eq 2).

$$2RAlMe_2 + 4Me_3SnF \rightarrow [RAlF(\mu\text{-}F)]_2 + 4SnMe_4 \quad (1)$$

$$RAlMe_2 + 2I_2 \rightarrow RAlI_2 + 2MeI \quad (2)$$

Unlike trimeric aminoalane difluoride [(2,6-*i*-Pr$_2$-C$_6$H$_3$)N(SiMe$_3$)AlF$_2$]$_3$[19] and [(Me$_3$Si)$_3$CAlF$_2$]$_3$,[20] compound **5** is a dimer in the solid state, as demonstrated by X-ray crystallography. Compound **5** is the first example of a dimeric aluminum difluoride.

Dynamic Behavior of 5. The ^{19}F NMR spectra of **5** at room temperature in C$_6$D$_6$ and toluene-*d*$_8$ both show only one broad singlet, indicating rapid exchange of the bridging and terminal fluorine atoms. This intramolecular exchange was also observed for the previously reported compounds [(2,6-*i*-Pr$_2$C$_6$H$_3$)N(SiMe$_3$)AlF$_2$]$_3$ and [(Me$_3$Si)$_3$CAlF$_2$]$_3$. When a solution of **5** in toluene-*d*$_8$ was cooled below 213 K (to 193 K), there are five separated signals in the ^{19}F NMR spectrum (δ −159.69 ppm (t, J = 15.0 Hz), −158.36 (t, J = 13.4 Hz), −141.13 (d, J = 82.4 Hz), −133.29 (s), −120.61 (d, J = 81.9 Hz)) in an intensity ratio of 2:3:1:3:1. Herein, assignment of the two signals (−159.69 and −158.36 ppm) to the bridging F atoms and the others to the terminal F atoms seems reasonable due to the large coupling constant difference of the two groups of signals as well as their correct integration (2:2). The ambient ^{1}H NMR spectrum of **5** exhibits only one broad singlet for SiMe$_3$ and one singlet for NSiMe$_3$ in toluene-*d*$_8$. When the solution was cooled to 273 K, the singlet for SiMe$_3$ becomes broad and separates into two singlets at 253 K. The singlet for NSiMe$_3$ and SiMe$_3$, respectively, at ambient temperature gives two separated singlets for SiMe$_3$ and two for NSiMe$_3$ (213 K). On the basis of the ^{1}H NMR data for SiMe$_3$ at 193 K (0.62 and 0.31 ppm, respectively), we conclude that a change in the ligand backbone takes place due to the quite different chemical shifts. Thus rapid dissociation/association of the Al−C bonds was also responsible for the fluxional process of **5** in solution. This dynamic process achieves an equilibrium at 213 K, giving a mixture of five- and four-coordinated species, while the [Al−(μ-F)]$_2$ core is maintained at this temperature. The broadening of the singlet at 0.31 ppm for SiMe$_3$ was probably due to the formation of four-coordinated species containing the C=C bond. The dissociation/association process is rapid at ambient temperature; therefore only one singlet can be observed for the SiMe$_3$ group on the NMR time scale. This assumption was further supported by the splitting of the Ph group signals into two sets in the ^{1}H NMR spectrum at low temperature. This M−C cleavage mechanism was also reported for compounds (ClMR)$_2$ (M = Sn, Pb; R = [N(SiMe$_3$)C(Ph)C(SiMe$_3$)$_2$]$^-$).[9]

(19) Waezsada, S. D.; Liu, F.-Q.; Murphy, E. F.; Roesky, H. W.; Teichert, M.; Uson, I.; Schmidt, H.-G.; Albers, T.; Parisini, E.; Nolte-meyer, M. *Organometallics* **1997**, *16*, 1260.
(20) Schnitter, C.; Klimek, K.; Roesky, H. W.; Albers, T.; Schmidt, H.-G.; Röpken, C.; Parisini, E. *Organometallics* **1998**, *17*, 2249.

Figure 1. Molecular structure of **5** in the crystal. Hydrogen atoms and solvent molecules have been omitted for clarity.

Compounds **1**−**8** have been fully characterized by ^{1}H NMR and ^{13}C NMR as well as elemental analyses (see Experimental Section). It is interesting to note that the ^{13}C chemical shifts of CN in compounds **2** and **3** are significantly higher than those found in compounds **7** and **8**, representing the most typical characteristics of η^3-chelating mode of the ligand in these compounds due to the delocalization of the electrons in the backbone of the ligand. ^{27}Al NMR and MS spectra demonstrate that compounds **1**−**4** and **6** are 4-fold coordinated at the aluminum centers in solution and monomers in the gas phase, respectively.

Molecular Structure of [RAlF(μ-F)]$_2$ (5). Molecular structure of **5** was determined by X-ray diffraction. Single crystals suitable for analysis were obtained from *n*-hexane/toluene at −20 °C. The structure of **5** with the atom-labeling scheme is shown in Figure 1. Selected bond distances and angles are listed in Table 3. Compound **5** adopts a dimeric structure in which the two bridging F atoms link two RAlF units in a planar four-membered ring (Al(1)−F(2)−Al(2)−F(3), the mean deviation of the ring, Δ = 0.0002 Å) and has approximately C_2 symmetry, as the bridging F(2) and F(3) reside on a 2-fold axis. Thus, each Al center is bonded to an η^3-chelating R ligand, one terminal F atom, and two bridging F atoms, resulting in three fused four-membered rings (Al(1)−C(2)−C(1)−N(1), Δ = 0.0052 Å; Al(1)−F(2)−Al(2)−F(3), Δ = 0.0002 Å; Al(2)−C(4)−C(3)−C(2), Δ = 0.0431 Å).

An important structural feature is the observation that every Al atom is pentacoordinated and the geometry of each aluminum coordination sphere can best be described as a distorted trigonal-bipyramid (tbp). A terminal F, a bridging F(3) atom, and a C(2) or C(4) atom reside in the equatorial plane with bond distances to Al on average of 1.668, 1.835, and 2.053 Å, respectively. The Al atom lies almost exactly in this plane with a negligible displacement. The sum of bond angles involving Al in this plane is 359.33° for Al(1) or 359.66° for Al(2), the angle F(1)−Al(1)−F(3) (102.23(15)°) or F(3)−Al(2)−F(4) (102.56(15)°) is significantly smaller than the angle F(3)−Al(1)−C(2) (142.2°) or F(3)−Al(2)−C(4) (137.1°), resulting from crowded environments around C(2) or C(4). The apical positions of this array are occupied by the bridging F(2) atom for both tbp geometries and the N(1) for Al(1) or N(2) for Al(2) with a bond angle of N(1)−Al(1)−F(2) of 152.4(2)° or N(2)−Al(2)−F(2) of 153.6(2)°. The deviation of the apical axis

Table 2. Selected Bond Lengths (Å) and Angles (deg) for Complexes 3 and 8

RAlCl$_2$ (3)

Al(1)−N(1)	1.918(2)	Al(1)−C(2)	2.015(3)	Al(1)−C(1)	2.334(3)
Al(1)−Cl(1)	2.1321(10)	Al(1)−Cl(2)	2.1276	C(1)−C(2)	1.498(3)
C(1)−N(1)	1.314(3)	N(1)−Si(1)	1.800(2)	C(2)−Si(2)	1.902(3)
C(2)−Si(3)	1.903	C(1)−C(3)	1.484(4)		
N(1)−Al(1)−C(2)	73.68(10)	N(1)−Al(1)−Cl(2)	113.05(7)	C(2)−Al(1)−Cl(2)	124.28(8)
N(1)−Al(1)−Cl(1)	114.57(7)	C(2)−Al(1)−Cl(1)	120.70(8)	Cl(2)−Al(1)−Cl(1)	106.53(4)
C(1)−N(1)−Si(1)	132.1(2)	Al(1)−N(1)−Si(1)	136.76	C(1)−C(2)−Si(2)	112.0(2)
C(1)−C(2)−Si(3)	117.1(2)	Al(1)−C(2)−Si(2)	118.75(13)	Al(1)−C(2)−Si(3)	108.84(12)
N(1)−C(1)−C(2)	113.9(2)	N(1)−C(1)−C(3)	122.1(2)	C(2)−C(1)−C(3)	123.9(2)

RAlCl$_2$(THF) (8)

Al(1)−N(1)	1.806(3)	Al(1)−O(1)	1.872(3)	Al(1)−Cl(1)	2.135(2)
Al(1)−Cl(2)	2.134(2)	N(1)−C(1)	1.450(5)	C(1)−C(2)	1.356(6)
C(2)−Si(1)	1.888(4)	C(2)−Si(2)	1.891(5)	C(1)−C(3)	1.507
N(1)−O(1)−Al(1)	109.0(2)	N(1)−Al(1)−Cl(2)	118.98(13)	O(1)−Al(1)−Cl(2)	99.61(11)
N(1)−Al(1)−Cl(1)	114.00(12)	O(1)−Al(1)−Cl(1)	102.64(11)	Cl(2)−Al(1)−Cl(1)	110.34(8)
Al(1)−N(1)−C(1)	117.7(2)	N(1)−C(1)−C(2)	124.9(4)	N(1)−C(1)−C(3)	112.8(4)
C(2)−C(1)−C(3)	122.3(4)	C(1)−C(2)−Si(2)	123.3(3)	C(1)−C(2)−Si(1)	120.8(3)

Table 3. Selected Bond Lengths and Angles for Complex [RAlF(μ-F)]$_2$ (5)

Al(1)−F(1)	1.665(3)	Al(1)−F(2)	1.837(3)	Al(1)−F(3)	1.841(3)
Al(1)−N(1)	1.977(4)	Al(1)−C(2)	2.051(5)	C(1)−C(2)	1.486(6)
C(1)−N(1)	1.308(6)	Al(2)−F(4)	1.670(3)	Al(2)−F(2)	1.850(3)
Al(2)−F(3)	1.829(3)	Al(2)−N(2)	1.964(4)	Al(2)−C(4)	2.055(5)
C(4)−C(3)	1.480(7)	C(3)−N(2)	1.312(6)	C(1)−C(71)	1.508(6)
C(3)−C(81)	1.504(7)	Al(1)−Al(2)	2.902(2)		
F(1)−Al(1)−F(2)	101.40(14)	F(1)−Al(1)−F(3)	102.23(15)	F(2)−Al(1)−F(3)	75.86(13)
F(1)−Al(1)−N(1)	105.6(2)	F(2)−Al(1)−N(1)	152.4(2)	F(3)−Al(1)−N(1)	92.7(2)
F(1)−Al(1)−C(2)	114.9(2)	F(2)−Al(1)−C(2)	102.5	F(3)−Al(1)−C(2)	142.2(2)
N(1)−Al(1)−C(2)	71.3(2)	Al(1)−F(2)−Al(2)	103.81(14)	Al(1)−F(3)−Al(2)	104.52(15)
F(4)−Al(2)−F(3)	102.56(15)	F(4)−Al(2)−F(2)	99.10(15)	F(3)−Al(2)−F(2)	75.81(12)
F(4)−Al(2)−N(2)	106.6(2)	F(3)−Al(2)−N(2)	92.6(2)	F(2)−Al(2)−N(2)	153.6(2)
F(4)−Al(2)−C(4)	120.0(2)	F(3)−Al(2)−C(4)	137.1(2)	F(2)−Al(2)−C(4)	100.9(2)
N(1)−C(1)−C(2)	114.2(4)	Al(1)−N(1)−C(1)	91.1(3)	Al(1)−C(2)−C(1)	83.4(3)
N(2)−C(3)−C(4)	114.2(4)	Al(2)−N(2)−C(3)	90.8(3)	Al(2)−C(4)−C(3)	82.8(3)
N(2)−Al(2)−C(4)	71.4				
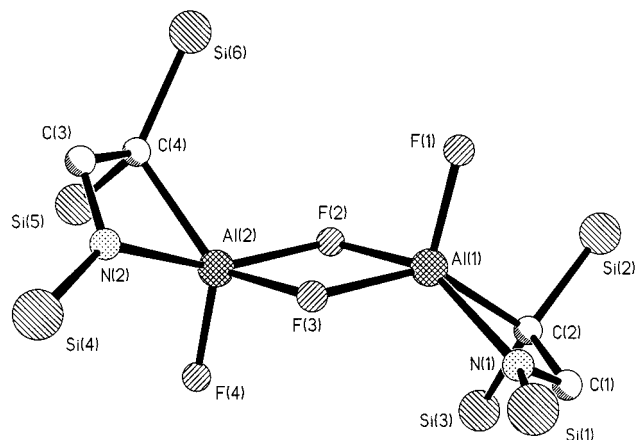
Figure 2. Central core of **5** in the crystal. Carbon atoms except for those in the ligand backbones have been omitted for clarity.

N(1)−F(2) is 13.8°, arising from the constraints caused by the specific angles in the chelating bidentate monoanionic ligand (average 71.4°) as well as in the acute F(2)−Al−F(3) angles of average 75.84° in the (μ-F)$_2$Al$_2$ ring (Figure 2).

The most unique and interesting feature in this structure is that the bridging F(2) and F(3) atoms connect the two units in such a way that F(2) occupies the same apical position and F(3) lies in the same equatorial position in the two tbp coordination spheres, resulting in a slightly longer Al−F(2) distance (average 1.844 Å) than Al−F(3) (average 1.836 Å). The distance of Al(1)−F(2) (1.837(3) Å) is shorter than Al(2)−F(2)

(1.850(3) Å), leading to a longer Al(1)−N(1) distance (1.977(4) Å) than Al(2)−N(2) (1.964(4) Å), and to the slightly unequal environments about Al(1) and Al(2). The N(1)−Al(1)−C(2) or N(2)−Al(2)−C(4) angle is very acute (average 71.3°), which is slightly smaller than that found in compound **3** (73.7°) because of the different coordination number at Al atoms of the two compounds. The acute angles of F(2)−Al(1)−F(3) and F(2)−Al(2)−F(3) (75.86° and 75.81°) lead to a rather long Al−Al distance (2.902 Å). Compared to compound **3**, the Al−N (1.971 Å) and Al−C (2.053 Å) bond lengths in the chelating plane are longer than those observed in **3** (Al−N, 1.918 Å; Al−C, 2.015 Å). The Al−F average distance (bridging, 1.839 Å) is in line with those found in compound [(Cp*AlF)$_2$SiPh$_2$]$_2$ (average 1.846 Å)[19] and slightly longer than those found by electron diffraction for (Me$_2$AlF)$_4$ (1.808 Å)[21] or by X-ray diffraction for [(Me$_3$Si)$_3$CAlF$_2$]$_3$ (1.785−1.815 Å)[20] and for [(2,6-*i*-Pr$_2$C$_6$H$_3$)N(SiMe$_3$)AlF$_2$]$_3$ (1.770−1.815 Å).[19] The terminal Al−F distances are 1.665 Å (Al(1)−F(1)) and 1.670 Å (Al(2)−F(4)) and are somewhat longer than those observed in [(2,6-*i*-Pr$_2$C$_6$H$_3$)N(SiMe$_3$)AlF$_2$]$_3$ (1.634−1.642 Å) and AlF$_3$ (1.63 Å)[22] determined by electron diffraction due to the higher coordination number of aluminum in compound **5**. No examples of five-coordinated aluminum compounds containing either bridging or terminal F atoms can be found in the literature for comparison.

(21) Gundersen, G.; Haugen, T.; Haaland, A. *J. Chem. Soc., Chem. Commun.* **1972**, 708.

(22) Shanmugasunderan, G.; Nagarajan, G. *Z. Phys. Chem.* **1969**, *240*, 363.

(23) Ergezinger, C.; Weller, F.; Dehnicke, K. *Z. Naturforsch.* **1988**, *43b*, 1621.
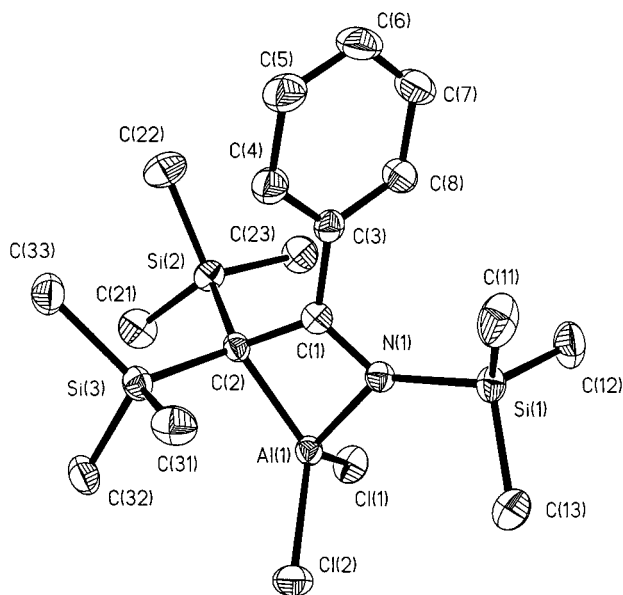
Figure 3. Molecular structure of **3** in the crystal. Hydrogen atoms have been omitted for clarity.

X-ray Crystallographic Analyses of Compounds 3 and 8. Crystal data for compounds **3** and **8** are summarized in Table 1, refinement details are discussed in the Experimental Section, and selected bond distances and angles are collected in Table 2. Single crystals of compounds **3** and **8** suitable for X-ray diffraction analyses were obtained by recrystallization from *n*-hexane at −8 °C. The molecular geometries and atom-labeling schemes are shown in Figures 3 and 4. Compound **3** adopts a distorted tetrahedral structure (Figure 3). The core angle (N(1)−Al(1)−C(2)) is acute (73.68°), which is compensated for by opening of the N−Al−Cl and C−Al−Cl angles. The structure of **3** is similar to that of the reported amidinate aluminum dichloride Ph−C(NSiMe₃)₂AlCl₂.[23] Because the chelating backbones in the two compounds are different, some differences in the structures are obvious: (1) The core angle N(1)−Al(1)−C(2) (73.68(10)°) is slightly larger than N−Al−N (72.9°) in compound Ph−C(NSiMe₃)₂-AlCl₂; (2) the Al(2)−C(2)−Si(2,3) (118.75(13)° and 108.84(12)°) angles in **3** are significantly smaller than the Al−N−Si angles in Ph−C(NSiMe₃)₂AlCl₂ (average 139°), indicating that R is more shielding than the amidinate.

The structure of compound **8** was also determined by X-ray crystallography for comparison (Figure 4). Interestingly, in the monomeric molecule of **8**, the geometry of the aluminum coordination sphere is also distorted tetrahedral, while the aluminum atom is surrounded by two chlorine atoms, one oxygen atom, and one nitrogen atom. The ligand R in this compound is, in contrast to **3**, monohapto (η^1) coordinated. The Al(1)−N(1) distance (1.806 Å) in **8** is much shorter than that in compound **3** (1.92 Å). The distinct bonding modes in **3** and **8** are also reflected in the different bond distances in the backbone of the ligand (long C(1)−N(1) and short C(1)=C(2) distances for **8** versus short C(1)−N(1) and long C(1)−C(2) contacts for **3**, Table 2). The long C(1)−C(2) and short C(1)−N(1) distances in compound **3** are indications of the delocalization of the electrons in the
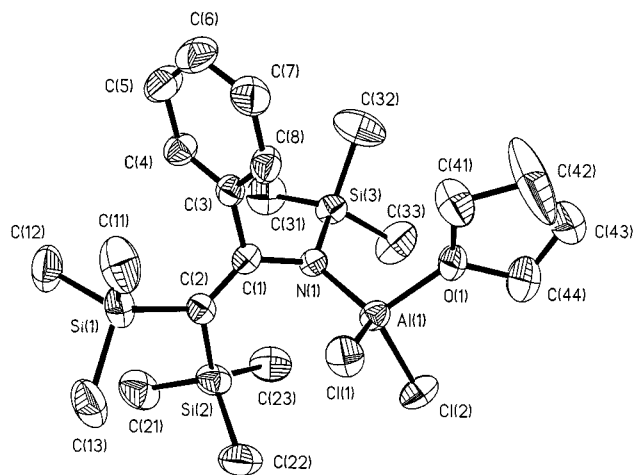
Figure 4. Molecular structure of **8** in the crystal. Hydrogen atoms have been omitted for clarity.

N(1)−C(1)−C(2) unit. The Al−Cl distances are comparable to those of compound **3**, while the Cl−Al−Cl angle (110.34(8)°) is slightly larger than that of compound **3** (106.53(4)°), reflecting the greater steric demand for η^3-chelating mode even though a THF molecule is coordinated to Al in compound **8**. The Al−O distance (1.872(3) Å) is in agreement with that observed for the stable compound (Me₃Si)₃CAlCl₂(THF) (1.887 Å).[20] Although in the solid state the THF in compound **8** seems as tightly coordinated to the aluminum center as that in (Me₃Si)₃CAlCl₂(THF) by the analysis of Al−O bond lengths in the two compounds, the instability of this compound is obviously due to easy removal of the THF molecule in vacuo. Thus, the bonding fashion of the ligand changes from η^1 to η^3 so as to stabilize the AlCl₂ unit (Scheme 2). The distances between Al(1) and C(1) as well as Al(1) and C(2) are 2.792 and 3.495 Å, respectively, which are in the range of van der Waals interaction, indicating that the C(1)=C(2) bond is not free in the solid state. In line with this observation, there is observed only one signal for the two SiMe₃ on C(2) in the ¹H NMR spectrum of **8** in C₆D₆ at ambient temperature, and the ¹³C NMR signal for C(2) is significantly downfield compared with those for C in compounds with normal C=C bonds. The ²⁷Al NMR spectrum showed a broad signal (62.66 ppm), which is low field shifted compared to the compounds of coordination number four described herein, indicating more electron density on the Al(1) and partial interactions between Al(1) and the C(1)=C(2) bond in solution. This may result from the Lewis acidic aluminum center containing four electron-withdrawing groups, leading to the flexibility of the C(1)=C(2) bond and the rotation of the two SiMe₃ groups around the C(1)=C(2) bond.

Supporting Information Available: Listings of crystal data, atom coordinates, and equivalent isotropic displacement parameters for all non-hydrogen atoms, hydrogen positional and thermal parameters, anisotropic displacement parameters, and bond distances and angles for compounds **3**, **5**, and **8**. This material is available free of charge via the Internet at http://pubs.acs.org.